

# Frequency comb swept lasers

Tsung-Han Tsai<sup>1</sup>, Chao Zhou<sup>1</sup>, Desmond C. Adler<sup>1</sup>, and James G. Fujimoto<sup>1\*</sup>

<sup>1</sup>Department of Electrical Engineering and Computer Science and Research Laboratory of Electronics, Massachusetts Institute of Technology, Cambridge, Massachusetts 02139, USA

\*jgf@mit.edu

**Abstract:** We demonstrate a frequency comb (FC) swept laser and a frequency comb Fourier domain mode locked (FC-FDML) laser for applications in optical coherence tomography (OCT). The fiber-based FC swept lasers operate at a sweep rate of 1kHz and 120kHz, respectively over a 135nm tuning range centered at 1310nm with average output powers of 50mW. A 25GHz free spectral range frequency comb filter in the swept lasers causes the lasers to generate a series of well defined frequency steps. The narrow bandwidth (0.015nm) of the frequency comb filter enables a ~-1.2dB sensitivity roll off over ~3mm range, compared to conventional swept source and FDML lasers which have -10dB and -5dB roll offs, respectively. Measurements at very long ranges are possible with minimal sensitivity loss, however reflections from outside the principal measurement range of 0-3mm appear aliased back into the principal range. In addition, the frequency comb output from the lasers are equally spaced in frequency (linear in k-space). The filtered laser output can be used to self-clock the OCT interference signal sampling, enabling direct fast Fourier transformation of the fringe signals, without the need for fringe recalibration procedures. The design and operation principles of FC swept lasers are discussed and designs for short cavity lasers for OCT and interferometric measurement applications are proposed.

©2009 Optical Society of America

**OCIS codes:** (110.4500) Optical coherence tomography; (120.3180) Interferometry; (140.3510) Lasers, fiber; (140.3600) Lasers, tunable.

---

## References and Links

1. D. Huang, E. A. Swanson, C. P. Lin, J. S. Schuman, W. G. Stinson, W. Chang, M. R. Hee, T. Flotte, K. Gregory, C. A. Puliafito, and J. G. Fujimoto, "Optical coherence tomography," *Science* **254**(5035), 1178–1181 (1991).
2. A. F. Fercher, C. K. Hitzenberger, G. Kamp, and S. Y. Elzaiat, "Measurement of Intraocular Distances by Backscattering Spectral Interferometry," *Opt. Commun.* **117**(1-2), 43–48 (1995).
3. S. R. Chinn, E. A. Swanson, and J. G. Fujimoto, "Optical coherence tomography using a frequency-tunable optical source," *Opt. Lett.* **22**(5), 340–342 (1997).
4. B. Golubovic, B. E. Bouma, G. J. Tearney, and J. G. Fujimoto, "Optical frequency-domain reflectometry using rapid wavelength tuning of a Cr(4+):forsterite laser," *Opt. Lett.* **22**(22), 1704–1706 (1997).
5. F. Lexer, C. K. Hitzenberger, A. F. Fercher, and M. Kulhavy, "Wavelength-tuning interferometry of intraocular distances," *Appl. Opt.* **36**(25), 6548–6553 (1997).
6. S. H. Yun, C. Boudoux, G. J. Tearney, and B. E. Bouma, "High-speed wavelength-swept semiconductor laser with a polygon-scanner-based wavelength filter," *Opt. Lett.* **28**(20), 1981–1983 (2003).
7. S. H. Yun, G. J. Tearney, J. F. de Boer, N. Iftimia, and B. E. Bouma, "High-speed optical frequency-domain imaging," *Opt. Express* **11**(22), 2953–2963 (2003).
8. M. A. Choma, K. Hsu, and J. A. Izatt, "Swept source optical coherence tomography using an all-fiber 1300-nm ring laser source," *J. Biomed. Opt.* **10**(044009), (2005).
9. R. Huber, M. Wojtkowski, J. G. Fujimoto, J. Y. Jiang, and A. E. Cable, "Three-dimensional and C-mode OCT imaging with a compact, frequency swept laser source at 1300 nm," *Opt. Express* **13**(26), 10523–10538 (2005).
10. R. Huber, M. Wojtkowski, K. Taira, J. G. Fujimoto, and K. Hsu, "Amplified, frequency swept lasers for frequency domain reflectometry and OCT imaging: design and scaling principles," *Opt. Express* **13**(9), 3513–3528 (2005).
11. W. Y. Oh, S. H. Yun, G. J. Tearney, and B. E. Bouma, "115 kHz tuning repetition rate ultrahigh-speed wavelength-swept semiconductor laser," *Opt. Lett.* **30**(23), 3159–3161 (2005).

12. Y. Yasuno, V. D. Madjarova, S. Makita, M. Akiba, A. Morosawa, C. Chong, T. Sakai, K. P. Chan, M. Itoh, and T. Yatagai, "Three-dimensional and high-speed swept-source optical coherence tomography for in vivo investigation of human anterior eye segments," *Opt. Express* **13**(26), 10652–10664 (2005).
13. S. Yun, G. Tearney, B. Bouma, B. Park, and J. de Boer, "High-speed spectral-domain optical coherence tomography at 1.3  $\mu\text{m}$  wavelength," *Opt. Express* **11**(26), 3598–3604 (2003).
14. K. Takada, "Fiber-optic frequency encoder for high-resolution OFDR," *IEEE Photonics Tech. Lett.* **4**(10), 1174–1177 (1992).
15. R. Passy, N. Gisin, J. P. von der Weid, and H. H. Gilgen, "Experimental and theoretical investigations of coherent OFDR with semiconductor laser sources," *J. Lightwave Technol.* **12**(9), 1622–1630 (1994).
16. S. Moon, and D. Y. Kim, "Normalization detection scheme for high-speed optical frequency-domain imaging and reflectometry," *Opt. Express* **15**(23), 15129–15146 (2007).
17. R. Huber, D. C. Adler, and J. G. Fujimoto, "Buffered Fourier domain mode locking: Unidirectional swept laser sources for optical coherence tomography imaging at 370,000 lines/s," *Opt. Lett.* **31**(20), 2975–2977 (2006).
18. R. Huber, M. Wojtkowski, and J. G. Fujimoto, "Fourier Domain Mode Locking (FDML): A new laser operating regime and applications for optical coherence tomography," *Opt. Express* **14**(8), 3225–3237 (2006).
19. D. C. Adler, Y. Chen, R. Huber, J. Schmitt, J. Connolly, and J. G. Fujimoto, "Three-dimensional endomicroscopy using optical coherence tomography," *Nat. Photonics* **1**(12), 709–716 (2007).
20. D. C. Adler, S.-W. Huang, R. Huber, and J. G. Fujimoto, "Photothermal detection of gold nanoparticles using phase-sensitive optical coherence tomography," *Opt. Express* **16**(7), 4376–4393 (2008).
21. C. M. Eigenwillig, B. R. Biedermann, G. Palte, and R. Huber, "K-space linear Fourier domain mode locked laser and applications for optical coherence tomography," *Opt. Express* **16**(12), 8916–8937 (2008).
22. M. Y. Jeon, J. Zhang, and Z. Chen, "Characterization of Fourier domain mode-locked wavelength swept laser for optical coherence tomography imaging," *Opt. Express* **16**(6), 3727–3737 (2008).
23. T. Amano, H. Hiro-Oka, D. Choi, H. Furukawa, F. Kano, M. Takeda, M. Nakanishi, K. Shimizu, and K. Ohbayashi, "Optical frequency-domain reflectometry with a rapid wavelength-scanning superstructure-grating distributed Bragg reflector laser," *Appl. Opt.* **44**(5), 808–816 (2005).
24. T. Bajraszewski, M. Wojtkowski, M. Szkulmowski, A. Szkulmowska, R. Huber, and A. Kowalczyk, "Improved spectral optical coherence tomography using optical frequency comb," *Opt. Express* **16**(6), 4163–4176 (2008).
25. E. J. Jung, J.-S. Park, M. Y. Jeong, C.-S. Kim, T. J. Eom, B.-A. Yu, S. Gee, J. Lee, and M. K. Kim, "Spectrally-sampled OCT for sensitivity improvement from limited optical power," *Opt. Express* **16**(22), 17457–17467 (2008).
26. T. R. Schibli, I. Hartl, D. C. Yost, M. J. Martin, A. Marcinkevicius, M. E. Fermann, and J. Ye, "Optical frequency comb with submillihertz linewidth and more than 10 W average power," *Nat. Photonics* **2**(6), 355–359 (2008).

## 1. Introduction

Optical coherence tomography (OCT) generates cross-sectional and three dimensional images of tissues *in situ* with micron scale resolution by measuring time delay of backscattered or back reflected light [1]. The recent development of Fourier domain OCT techniques with spectrometer based system (spectral / Fourier domain OCT, or SD/FD-OCT) or frequency swept laser sources based system (swept source OCT or SS-OCT) enables imaging speeds 10 to 100 times faster than standard time domain OCT techniques [2–13]. Compared to SD/FD-OCT, SS-OCT can have improved overall sensitivity if operated in shot-noise-limit because there are no spectrometer losses and the photodetectors used are more sensitive than cameras [8, 14–16]. SS-OCT also enables operation at long wavelength ranges without the need for expensive InGaAs cameras. Improved system dynamic range can also be achieved in SS-OCT because it uses dual-balanced detection and higher bit depth data acquisition (DAQ) systems than cameras. In addition, swept source/Fourier domain detection can provide very large number of axial samples, as determined by the speed of DAQ system.

Typical swept lasers consist of a broadband gain medium with a tunable optical bandpass filter in the cavity. The tunable filter is swept so that the transmission frequency varies in time and sufficient time is needed to allow lasing in the transmission bandwidth to build up from spontaneous emission inside the cavity. This limits the maximum tuning rate of the laser and also results in lower power, broader instantaneous linewidth or shorter instantaneous coherence length. Fourier domain mode-locking (FDML) is a new mode of operation for frequency swept lasers that overcomes these problems and is especially promising for high speed OCT imaging [17, 18]. An FDML laser uses a cavity with a long fiber delay line and a fiber Fabry-Perot tunable filter (FFP-TF) whose sweep rate is synchronized with the round-trip time of light inside the cavity. The long fiber delay line stores the entire frequency sweep

inside the laser and the different frequencies in the sweep return to the FFP-TF at the time when the filter is tuned to transmit them. The laser generates a sequence of optical frequency sweeps at the cavity repetition rate. However, the coherence length of standard FDML lasers is limited by the bandwidth of the FFP-TF and a 5dB~10dB drop in sensitivity over a 3mm depth range is typically observed [19–22]. For OCT imaging applications, it is desirable to have uniform imaging sensitivity over a large depth range.

To improve the sensitivity roll off or ranging depth in OCT imaging systems, light sources with discrete frequency steps and narrow instantaneous bandwidth have been demonstrated. Amano *et al.* demonstrated 1550nm superstructure-grating distributed Bragg reflector (SSG DBR) laser with the bandwidth of a few MHz for SS-OCT imaging [23]; Bajrąszewski *et al.* used an external frequency comb filter with bandwidth of 1.62GHz to generate discrete frequency steps for SD-OCT imaging at 840nm [24]; Jung *et al.* also used an external fiber Sagnac comb filter to generate light with very narrow bandwidths [25]. These methods showed that the ranging depth of the OCT system can be increased by reducing the instantaneous bandwidth of the light source, suggesting the use of frequency comb techniques can improve the sensitivity over a longer ranging depth.

At the same time, most Fourier domain OCT systems require re-sampling or recalibrating the OCT interference fringe signals in order to provide data evenly sampled in frequency domain prior to fast Fourier transformation (FFT). This recalibration process is computationally expensive and limits the real-time operation of OCT. For SS-OCT, Eigenwillig *et al.* have successfully demonstrated an approach to linearize frequency sweeps in FDML lasers by incorporating the second and third harmonics of the drive waveform to FFP-TF [21]. However, this approach requires that the FFP-TF have a high frequency response and is also sensitive to thermal drift in the FFP-TF.

In this manuscript, we demonstrate frequency comb (FC) lasers, a new type of swept laser incorporating a fixed narrowband frequency comb fiber Fabry-Perot (FFP-FC) filter inside the cavity of conventional swept lasers and FDML lasers. FC swept lasers generate a sweep of discrete steps in frequency, rather than a continuous sweep. The extremely narrow bandwidth of the frequency steps generated by FC lasers improves the sensitivity roll off in OCT compared to conventional swept source and FDML lasers, enabling imaging over a longer depth range. The comb frequencies are equally separated in k-space, providing a clock signal which can be used to trigger the OCT interference fringe acquisition. This self-clocking method outperforms standard frequency calibration methods using reference Mach-Zehnder interferometer signals. The general design principles of FC lasers will also be discussed, which will be important for the design of future high speed, short cavity FC lasers.

## 2. Principles of frequency comb generation

In a conventional swept laser or FDML laser, the frequency is continuously varying during the sweep. In an FC laser, a fixed frequency comb filter FFP-FC with small free spectral range (FSR) and narrow transmission bandwidth is used in the cavity in addition to a tunable filter FFP-TF. The transmission function of the FFP-FC is defined as:

$$T = \frac{(1-R)^2}{1-2R \cdot \cos(2k \cdot L) + R^2}, \quad (1)$$

where  $R$  and  $L$  are the reflection coefficients and the cavity length in the Fabry-Perot resonator respectively and  $k$  is the wavevector of the incident light. This filter thus provides a series of transmission peaks with an equal frequency spacing of  $\Delta f = c/2nL$ , also known as the FSR. However it is important to note that if the material  $n$  in the Fabry-Perot resonator has dispersion, the transmission resonances will no longer be uniformly spaced. Figure 1 shows the operating principle of FC lasers. During operation, the FFP-TF is continuously tuned across the sweep range and frequency components which pass through both the FFP-TF

and FFP-FC filters can be amplified by the gain medium, while other frequency components are suppressed. The laser operates at frequencies given by the product of the transmissions of these two cascaded filters. As the FFP-TF is swept in time, the laser generates a series of fixed frequency steps with varying amplitudes. If the bandwidth of the tunable FFP-TF is less than the FSR of the frequency comb FFP-FC, the laser will generate only a single frequency at a time and the intensity output will be strongly modulated. If the bandwidth of the tunable FFP-TF is comparable to the FSR of FFP-FC, then the laser can operate in a superposition of FFP-FC frequencies and is partially modulated in intensity (Fig. 1 bottom). The instantaneous linewidth of the FC laser is determined by the bandwidth of FFP-FC, which is much narrower than the bandwidth of the FFP-TF. This produces a longer coherence length output because the laser tunes in a discrete series of steps each of which have narrow linewidth. This produces less sensitivity roll-off over large imaging depths compared to conventional swept lasers.

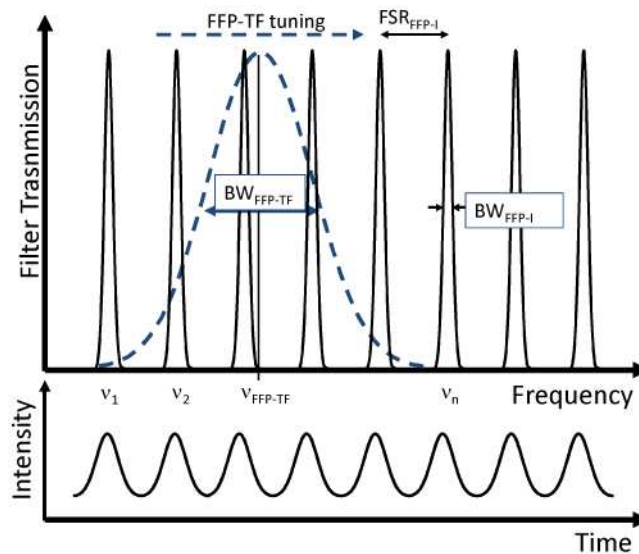


Fig. 1. Operating concept of a frequency comb swept laser.

Moreover, since the peaks in the intensity modulation are equally spaced in frequency, they can be used as a clock signal to sample the OCT interference signal. This results in a calibrated OCT interference signal which is equally sampled in  $k$ -space and can be directly Fourier transformed to obtain axial scan information. The OCT interferometric signal obtained using an FC laser can be considered as a discrete version of interferometric signal obtained using a standard FDML laser, and the discrete spacing is determined by the FSR of FFP-FC because it determines the frequency comb spacing of the laser.

However, an interferometric signal which has a frequency higher than one half of the sampling rate will be aliased. This means that OCT signals from reflections which are at a range larger than the principal range 0 to  $2nL$  are aliased so that the measurement appears at depths from 0 to  $2nL$ . The FSR of the frequency comb filter also determines the number of samples that can be generated as the laser is swept across its tuning range. Therefore, it is important to choose the FSR of the frequency comb filter FFP-FC so that the frequency comb spacing is small enough to provide a large enough measurement depth range and sufficient numbers of samples during the frequency sweep.

### 3. Methods

#### 3.1 Laser geometry

Figure 2 (a) shows a schematic diagram of the FC swept laser. The laser has a ring resonator geometry with a semiconductor optical amplifier (SOA, Covega, Inc.) gain medium, a tunable filter FFP-TF (Micron Optics, Inc.), and a fixed frequency filter FFP-FC (Micron Optics, Inc.) in a cavity with 15m physical path length (optical path length of 22.5m). The laser output is amplified with a second SOA (Covega, Inc.) outside the cavity which serves as a booster amplifier. The FFP-TF has a FSR of 200nm centered at 1,310nm and finesse of 2,000, while the FFP-FC has a FSR of 0.15nm at 1,310nm and finesse of 10. The ratio of the bandwidth of the FFP-TF to the FSR of the FFP-FC is 0.67. The FSR of FFP-FC is ~25GHz, corresponding to a maximum imaging depth of 3mm. A sinusoidal waveform of 1kHz was used to drive the FFP-TF. The average output power of the laser before the booster amplifier was 0.6 mW and after the booster was 40mW. Figure 2 (b) shows a schematic diagram of the FC-FDML laser, using the same FFP-TF and FFP-FC filter. The FFP-TF is driven with a sinusoidal waveform at 59.8427kHz, synchronous to the optical round-trip time of the 3,416m long cavity. A single buffered geometry [17] was used to double the frequency sweep rate to 119.6854kHz and the average output power before the booster amplifier was 1.6 mW and after the booster was 50mW. To compare performance, the frequency comb filter FFP-FC was removed from the cavities in Figs. 2 (a) and (b) to obtain conventional swept source and FDML laser operation. The output spectra of the lasers were monitored by a high speed oscilloscope and an optical spectrum analyzer via a 1% fiber coupler.

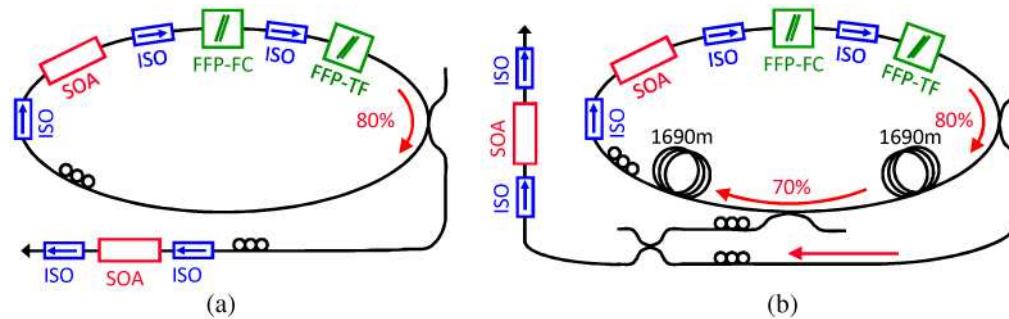


Fig. 2. Schematic diagrams of the frequency comb (FC) swept laser (a) and frequency comb Fourier domain mode-locked (FDML) laser (b).

#### 3.2 Point spread function measurement

The OCT system used to measure the point spread functions (PSFs) of these lasers is shown in Fig. 3. A small portion of the laser output was coupled to an asymmetric Mach-Zehnder interferometer (MZI) that produces interference fringes with zero crossing evenly spaced in frequency. The MZI fringes were detected by a dual-balanced photodetector and used to generate a clock to recalibrate the interference fringe signals from the OCT system. The OCT system consisted of a dual-balanced Michelson interferometer with a pair of optical circulators and a 50/50 fiber-optic splitter [17, 19]. The MZI and OCT fringes were recorded simultaneously using a high speed oscilloscope. The nonlinear frequency sweep in the OCT fringe data was recalibrated using the MZI fringe data and a fast Fourier transform was performed to obtain the PSFs.

#### 3.3 Sensitivity measurement

The instantaneous linewidth or instantaneous coherence length of the lasers were characterized by measuring the sensitivity for different interferometer delays. The power on

the sample reflector was 14mW. To characterize the sensitivity of conventional and FC swept lasers for OCT, a calibrated  $-56\text{dB}$  reflection was used. The reference arm power was attenuated to about 150 - 200 microwatts. The sensitivity was measured as the ratio between the peaks of the PSFs to the standard deviation of the noise floor, which was measured with the sample arm blocked. System losses of  $\sim 2.5\text{dB}$  arising from losses in the optics, mirror reflectivity, and backcoupling were subtracted from the measured sensitivity values.

### 3.4 Self-Clocking method

To test the feasibility of self-clocking, the A/D clocking process was simulated by post processing the OCT interference data. A portion of the output from the laser in Fig. 3 was detected by a photodetector to record the intensity modulation. A low pass filter at 200MHz was used on the photodetected signal to remove high frequency electronic noise. The filtered laser intensity output and OCT interference signals were recorded simultaneously using a high speed oscilloscope. The data was post processed using a custom MATLAB script to find the peak positions of the laser intensity output and sample the OCT interference signal at these times. In this case, with total tuning range of 135nm and 0.15nm FSR of the FFP-FC, there were about 900 peaks. The sampled OCT interference fringes were then zero-padded to 2048 points and directly Fourier transformed. Therefore, the final OCT A-line data contained 1024 points over the principal imaging range. No other calibration or dispersion compensation procedures were applied for the analysis of these data.

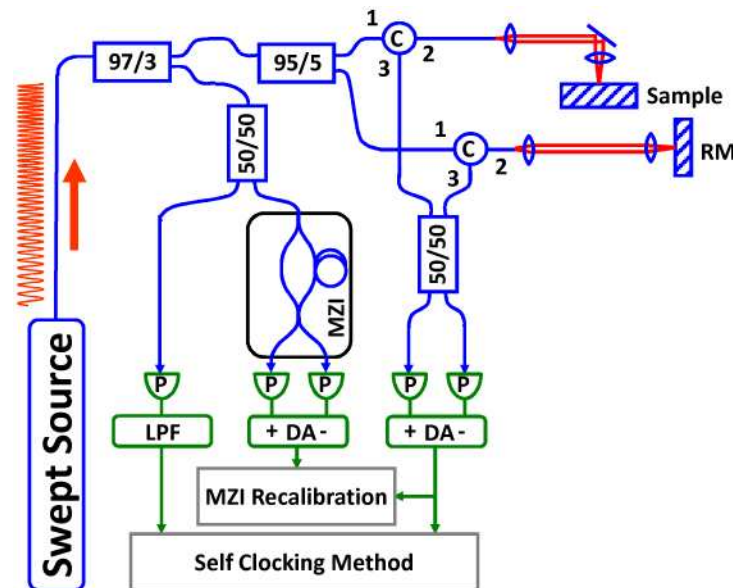


Fig. 3. Schematic of the swept source OCT system (optics: blue; electronics: green; recalibration clock mechanism: gray). C: circulator; MZI: Mach-Zehnder interferometer; RM: reference mirror; DA: differential amplifier; P: photodetector; LPF: lowpass filter.

## 4. Performance of FC swept lasers

### 4.1 Spectrum

Figure 4 shows the output spectra of the FC swept laser. The total tuning range of the spectrum is 135nm, with full width half maximum (FWHM) of 70nm. As mentioned in Section 3.1, the transmission bandwidth of FFP-FC is  $\sim 0.015\text{nm}$  at a center wavelength of 1310nm. Therefore, the frequency bandwidth of the individual frequency steps in the frequency comb cannot be resolved because of the limited resolution of the optical spectrum analyzer. The zoomed view in Fig. 4 (b) shows the  $\sim 0.15\text{nm}$  spacing between each frequency



step, corresponding to the FSR of the frequency comb filter FFP-FC. The background underneath the frequency modulation is produced by the amplified spontaneous emission (ASE) of the booster SOA.

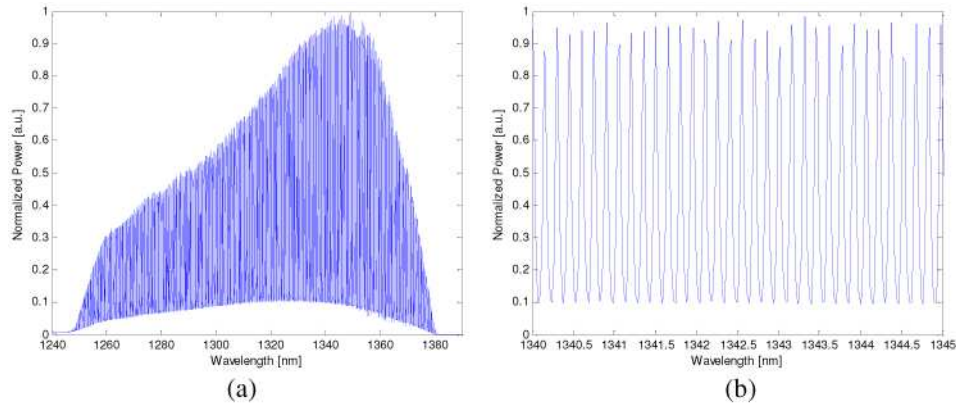


Fig. 4. (a) Output spectrum and (b) the zoomed view from 1340nm to 1345nm of the FC swept laser.

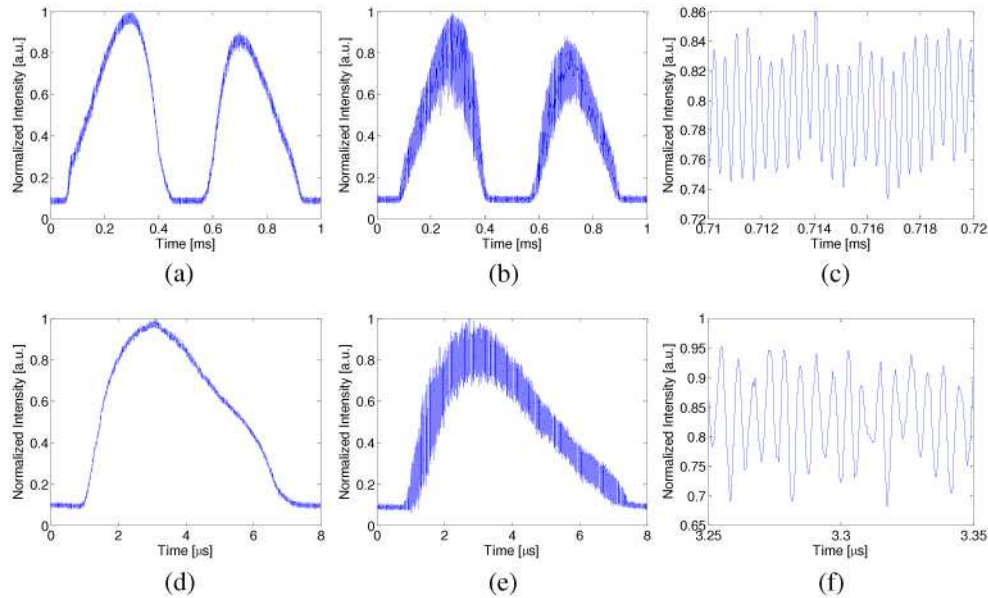


Fig. 5. Transient intensity output traces of different lasers: (a) conventional swept laser; (b) FC swept laser; (c) zoomed view from 0.71ms to 0.72ms of (b); (d) FDML laser; (e) FC-FDML laser; (f) zoom-in view from 3.25μs to 3.35μs of (e).

#### 4.2 Intensity output and interferometric fringe

Figure 5 compares transient intensity outputs of the conventional swept source, FDML and FC swept lasers. The zoomed view in Fig. 5(c) and (f) is similar to that predicted by Fig. 1(b). The frequency comb filter FFP-FC in the cavity generates a modulated intensity output. Each peak in the modulation represents an individual frequency step. The time spacing between each peak in the intensity is determined by the instantaneous tuning speed of FFP-TF. The time between peaks in central part of the frequency sweep is smaller than that in the edge of the sweep because the tunable filter FFP-TF is driven sinusoidally.

Figure 6 shows an example OCT interferometric signal at a delay of 0.7mm using the FC and FC-FDML lasers. The modulation in the laser output intensity can be seen superposed on the OCT interferometric signals. Each peak in the modulation represents an individual frequency step, indicating that the interference traces can be precisely calibrated to frequency (linear in k-space) if they are sampled at the peaks of the modulations.

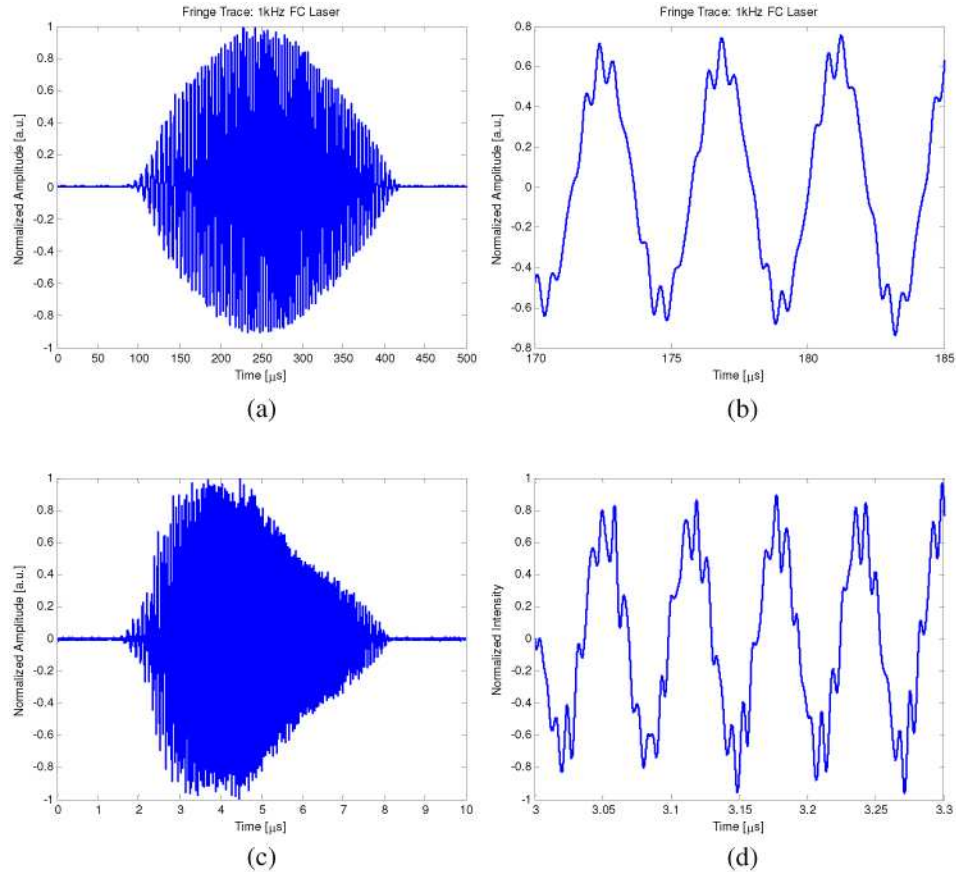


Fig. 6. OCT interferometric traces at 0.7mm imaging depth using a (a) FC swept laser and (c) FC-FDML laser. (b) and (d) are the zoomed views of (a) from 170μs to 185μs and (c) from 3μs and 3.3μs respectively.

#### 4.3 Sensitivity roll off comparison between conventional and FC swept laser

The sensitivity was measured using both conventional and FC swept lasers and was 108dB and 107.5dB respectively, indicating that adding the frequency comb filter inside the cavity did not degrade the system sensitivity. The point spread functions of the conventional and FC swept lasers were measured at different imaging depths from 0.1mm to 2.8mm. For comparison, the OCT interference traces of FC laser were recalibrated using MZI signal and the self-clocking method separately. From Fig. 7, the measured roll off is -10dB for the conventional swept laser versus -5dB for FC laser using the MZI recalibration method and only -1.2dB using the self-clocking method. Using the same MZI recalibration method, the FC laser shows less sensitivity roll off compared with the conventional swept laser, indicating the instantaneous coherence length of the frequency steps in the FC laser are longer. Furthermore, the self-clocking method calibrates the interference data to linear k-space more accurately compared to the MZI recalibration method, achieving much less sensitivity roll off over the 2.8mm imaging depth. The measured FWHM resolution of the point spread function



was  $11\mu\text{m}$  in air, which corresponds to  $\sim 8\mu\text{m}$  in tissue, while the theoretical value of the resolution was  $10.8\mu\text{m}$  in air. The measured resolution is slightly worse than the theoretical value because of several factors such as the electronic bandwidth limit of the detectors, spectral shape and residual sampling errors. The axial resolution using the FC swept laser is the same as that from conventional frequency swept and FDML lasers operating with the same bandwidth.

There are two causes contributing to the slightly elevated noise floor in Figs. 7 (b-c): (1) The output power of the FC swept lasers contains a portion of ASE from the post-amplified stage, as shown in Fig. 4. Hence, although the same output power from conventional and FC swept lasers was used to compare the sensitivity roll off, the actual amplitude of the interference signal using FC swept lasers was less than with conventional swept lasers. Note that the sensitivity in Figs. 7 is normalized, so the reduced amplitude of the point spread function using the FC swept lasers causes an elevated noise floor. (2) Also, in Figs. 7 (a-b), the PSFs were obtained from data sets with 2048 points, and thus may have lower noise levels compared with the data sets using the self-clocking method which contained 900 points.

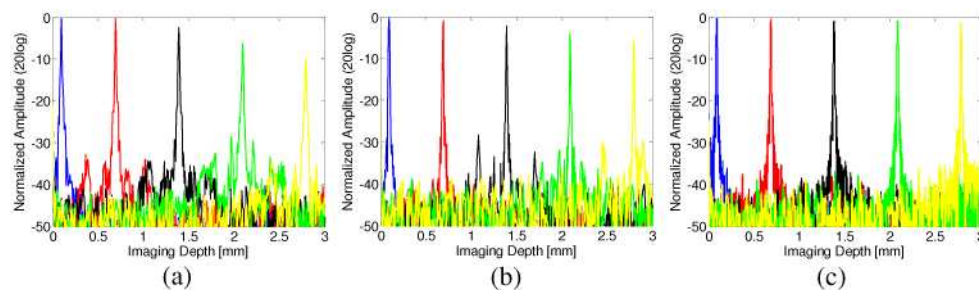


Fig. 7. Sensitivity roll off from 0.1mm to 2.8mm imaging depth: (a) conventional swept laser; (b) FC swept laser with MZI calibration; (c) FC swept laser with self-clocking calibration.

The same comparison was also performed between a FDML and FC-FDML laser. Figure 8 shows the sensitivity roll off over 2.8mm depth for an FDML laser, a FC-FDML laser with MZI recalibration, and a FC-FDML laser with self-clocking. The sensitivity using the FDML laser rolls off by  $-5\text{dB}$  which shows that the instantaneous linewidth of FDML laser is narrower than conventional swept laser. Using MZI recalibration, the sensitivity roll off of FC-FDML laser is  $-3\text{dB}$ , which is slightly improved compared to the standard FDML laser. However, using the self-clocking method, a sensitivity roll off of only  $-1.3\text{dB}$  can be achieved using the FC-FDML laser. Figures 8 (b-c) also show a slightly elevated noise floor as discussed previously. This result is consistent with previous section and shows that FC lasers have superior linewidth and coherence length performance compared with standard swept lasers or FDML lasers. Table 1 summarizes the sensitivity roll offs for all of the lasers.

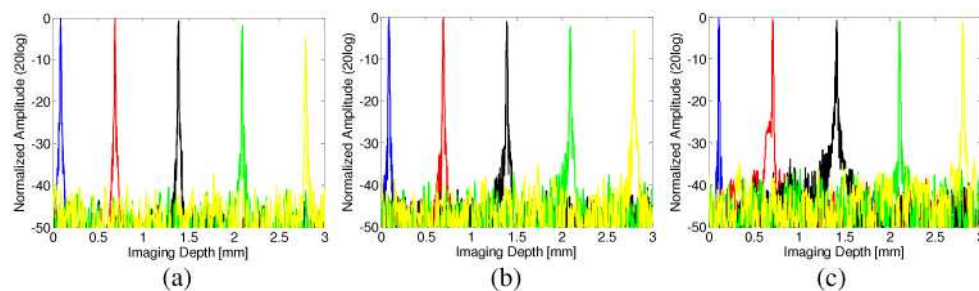


Fig. 8. Sensitivity roll off from 0.1mm to 2.8mm imaging depth: (a) FDML laser; (b) FC-FDML laser with MZI calibration; (c) FC-FDML laser with self-clocking calibration.

**Table 1. Summary of sensitivity roll off at 2.8mm imaging depth of different lasers.**

| Laser               | No FC filter | FC + MZI calibration | FC + Self-clocking |
|---------------------|--------------|----------------------|--------------------|
| Swept laser (1kHz)  | -10dB        | -5dB                 | -1.2dB             |
| FDML laser (120kHz) | -5dB         | -3dB                 | -1.3dB             |

#### 4.4 Frequency clocking and accuracy

Since the self-clocking method takes samples at every peak point of the intensity modulated output signal, any sampling errors, such as missing samples or timing jitter would cause the PSF to become broader and reduced in height. The FFT is very sensitive to sampling errors, especially when detecting longer delays where the OCT interferometric signal has higher oscillation frequency. Figure 9 shows an example of the software peak detection results from an intensity output trace of FC-FDML laser. As mentioned in Section 4.2, the time position of the peaks in the intensity modulation is determined by the instantaneous tuning speed of the filter which is driven by a sinusoidal waveform. The nonlinear instantaneous tuning speed can be seen in the peak positions shown in Fig. 9(a). Figure 9(b) shows the time intervals between the peaks and is a measure of the sampling error and timing jitter. The sampling timing jitter increases significantly at the beginning and end of the frequency sweep, where the laser output intensity is lower. However sampling errors at these times are less critical than during the central part of the sweep where the signal energy is higher. Timing jitter in the center of the sweep, where the signal powers are higher, can cause significant broadening of the PSF. It is also important that there are no missed samples. Missing a sample causes a time translation of all subsequent samples and will broaden the PSF. Applying a lowpass filter to the laser intensity output, as mentioned in Section 3.4, can eliminate high frequency electronic noise and reduce sampling errors. Reducing sampling timing jitter and errors is extremely important for achieving good PSF performance. This issue will require special attention for future system designs where the A/D is clocked using the modulated laser intensity output.

#### 4.5 Extended depth ranging

As mentioned above, aliasing occurs if the OCT signal is outside the principal measurement range set by the frequency comb filter FFP-FC. The same aliasing phenomenon was also reported by Jung *et al.* using a light source with an external frequency comb filter [25]. Figure 10(a) shows the PSF when reflection is at 0.06mm depth. Figure 10(b) shows a reflection from a depth of 5.94mm, which appears in the measurement as if it is at 0.06mm delay. Reflections at a position  $z$  between 3mm to 6mm range appear as if they are between 3mm to 0mm, at a position  $(3\text{mm} - z)$ , mirrored about the 3mm position. When the reflection is at the edge of the principal measurement range, 3mm in this case, the corresponding PSF

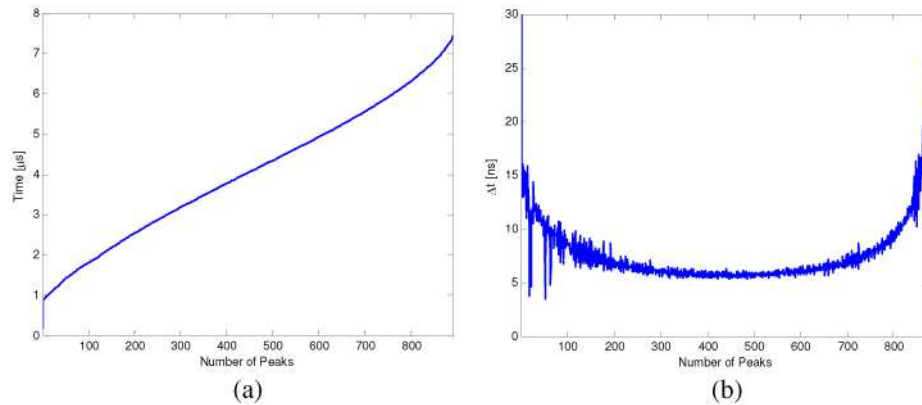


Fig. 9. (a) Time position of each peak found in the laser intensity modulation. (b) Time difference between each peak found in the intensity modulation. The horizontal axis indicates the peak numbers that were found by the peak-finding script.

and its mirror PSF would overlap and it would not be possible to distinguish if the reflection were from the edge of the imaging range or near zero delay. Figure 10(c) shows the PSF when the reflection is at 6.06mm. Because of the 25 GHz FSR of the frequency comb filter FFP-FC, the signal from a reflection at 6.06mm appears as if it is at 0.06mm depth because the measurement range repeats every 6mm. Reflections which are at a position  $z$  between 6mm to 9mm range appear as if they are between 0mm and 3mm, at a position  $(z - 6\text{mm})$ . Note that the sensitivity for the reflection at 6.06mm delay is decreased by only  $-1.5\text{dB}$ , demonstrating the narrow linewidth of the frequency steps generated by the FC laser. Although the aliasing occurs at deeper depths, this implies that it is possible to see signals at very long delays with very little loss of sensitivity. At the same time, imaging structures which extend over a very large range of depths would require techniques to remove aliasing. The large imaging depths could be very useful for applications such as profilometry, where the measured signals can be easily de-aliased.

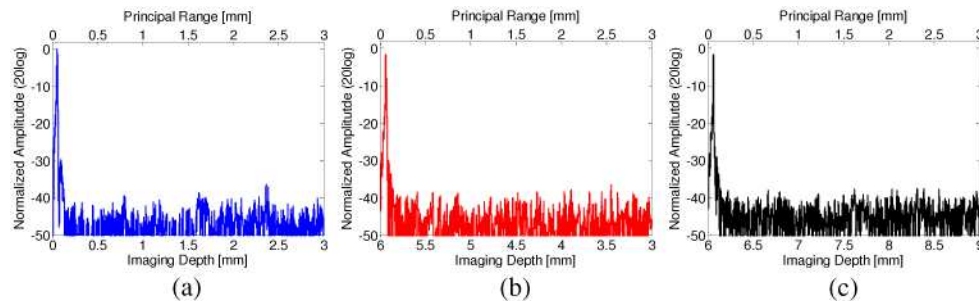


Fig. 10. Sensitivity roll off at imaging depth deeper than the principal imaging range. (a) Reflection is at 0.06mm depth. (b) Reflection is at 5.94mm depth. (c) Reflection is at 6.06mm. Each amplitude is normalized by the peak value in (a).

## 5. Discussion

### 5.1 Advantages of FC swept lasers

Frequency comb operation can improve performance for both conventional swept lasers as well as FDMR lasers. The frequency comb filter inside the laser cavity causes the laser to generate a sweep of frequency steps with narrow instantaneous linewidth, producing longer instantaneous coherence length output. As Section 4.3 shows, this property of FC swept lasers improves sensitivity roll off, enabling measurements over a longer depth range with both conventional swept and FDMR lasers.

The intensity modulation in the laser output also enables self-clocking to precisely sample the OCT interferometric signal into linear k-space (equal frequency intervals) without additional recalibration. Compared to typical MZI recalibration methods [19–22], using self-clocking achieves better sensitivity roll off. In addition, self-clocking should simplify the DAQ system requirements since a separate high speed channel is no longer required to detect an MZI signal. Moreover, precise sampling of the OCT interferometric data allows phase information to be recorded more accurately, which should enable FC lasers to achieve improved sensitivity for phase detection applications. The frequency comb filter FFP-FC could also be frequency locked to an external frequency standard if the generation of absolute frequencies are required. These approaches are somewhat analogous frequency comb methods that have been demonstrated with broadband femtosecond lasers [26].

FC lasers also dramatically improve the performance of conventional (non-FDML) swept lasers. As shown in Table 1, an FC swept laser can achieve a  $-5\text{dB}$  sensitivity roll off using MZI recalibration and  $-1.2\text{dB}$  sensitivity roll off using self-clocking, comparable to or better than conventional FDML lasers. Conventional swept lasers have the advantage that they are simpler than FDML lasers and can be operated at different sweep rates since they do not require synchronization of the sweep rate to the cavity round trip time.

### 5.2 Design principles for frequency comb swept lasers

FC swept lasers contain a (fixed) frequency comb filter FFP-FC and a tunable filter FFP-TF inside the cavity. The FSR of tunable FFP-TF must be wide enough to support the tuning range of the laser, which determines the axial resolution for OCT system. The FSR of frequency comb FFP-FC determines the frequency comb spacing and thus determines the principal measurement depth range before aliasing occurs. To produce a sweep with frequency steps as well as a stable modulation in the output intensity trace, the ratio of tunable FFP-TF bandwidth to frequency comb FFP-FC FSR should be less than 1. Hence, shorter frequency comb FSRs can give longer imaging ranges, but require tunable filters with higher finesse. The shorter FSR also means that the DAQ speed must be increased because the frequency steps occur faster. Tunable filters FFP-TF with higher finesse are often more difficult to fabricate and can have lower damage thresholds than tunable filters with lower finesse. In contrast, it is easier to achieve high finesse using a fixed frequency comb filter FFP-FC. The bandwidth of the frequency comb filter FFP-FC determines the instantaneous linewidth of the frequency steps or the instantaneous coherence length of the laser output.

To design a frequency comb swept laser, there are several basic principles that need to be considered: (1) the FSR of the (fixed) frequency comb FFP-FC filter determines the principal imaging depth and the number of samples in the frequency sweep. From Eq. (1), the FSR is determined by the optical cavity length of the FFP-FC, and the principal imaging depth is one half of the FFP cavity length; (2) The bandwidth of frequency comb FFP-FC determines the instantaneous linewidth of the frequency steps or the coherence length of the laser output; (3) The bandwidth of tunable FFP-TF should be less than the FSR of frequency comb FFP-FC in order to generate frequency steps and to produce intensity modulation; (4) the FSR of the tunable FFP-TF must be sufficient to support the frequency sweep bandwidth and determines the axial resolution for OCT imaging or interferometric measurement. There are also additional principles governing swept lasers: (5) for a non-FDML FC swept laser, the cavity length of the laser determines the maximum tuning rate of the laser, with shorter cavities enabling faster tuning [10,11]; (6) for the FC-FDML laser, the cavity length determines the sweep repetition rate and the tuning rate of the laser and the sweep repetition rate is fixed by the cavity length. The effective tuning rate can be multiplied by using buffered configurations [17]. Design principles (1) and (2) can determine the finesse of the frequency comb FFP-FC while (3) and (4) determine the finesse of the tunable FFP-TF required for the FC swept laser.

Figure 11 shows examples for general FC swept laser design. Figure 11(a) shows a standard laser with a tunable FFP (FFP-TF) and a frequency comb FFP (FFP-FC). Based on

the principles mentioned above, the parameters of FFP-TF and FFP-FC determine the principal imaging range and sensitivity roll off performance for OCT, while the laser cavity length  $L_c$  determines the maximum sweep rate of the laser.

In this paper we demonstrated a FC swept laser with a 15m cavity at 1kHz sweep rate with  $-1.2\text{dB}$  sensitivity roll off over 2.8mm depth. The sweep rates of FC swept lasers are expected to scale with roundtrip time. For conventional (non-FDML) swept lasers, several roundtrips are needed for each wavelength to allow lasing to build up from spontaneous emission [18], so that swept lasers with shorter cavity lengths have shorter roundtrip times and can achieve higher sweep speeds. By reducing the laser cavity length from 15m to 15cm, a factor of 100x, the sweep speed should increase from 1kHz to 100kHz. These short lengths are difficult to fabricate using optical fiber cavities, but can be achieved using bulk cavity designs.

In the limit where cavity lengths are very short, the longitudinal modes of the cavity become important. Figure 11(b) shows a laser with a short cavity length and a FFP-TF. When the laser cavity length is very short, the cavity itself can work analogously to a frequency comb FFP filter. In this case, the laser cavity length  $L_s$  not only determines the maximum tuning rate of the laser, but also sets the principal measurement depth as  $L_s/2$ . The laser linewidth is determined by a combination of the cavity output coupling and laser dynamics. When the tunable filter is swept, the laser generates a sweep of frequency steps which are the longitudinal modes of the laser cavity itself.

A complementary limit occurs in FDML lasers when the cavity length is very long, such that the longitudinal mode spacing is very small. Figure 11(c) shows an FDML laser with long dispersion managed delay and two FFPs. The parameters of the tunable FFP-TF and frequency comb FFP-FC determine the principal imaging range and sensitivity roll off performance for OCT, while the laser cavity length  $L_{\text{FDML}}$  determines the sweep rate of the laser.

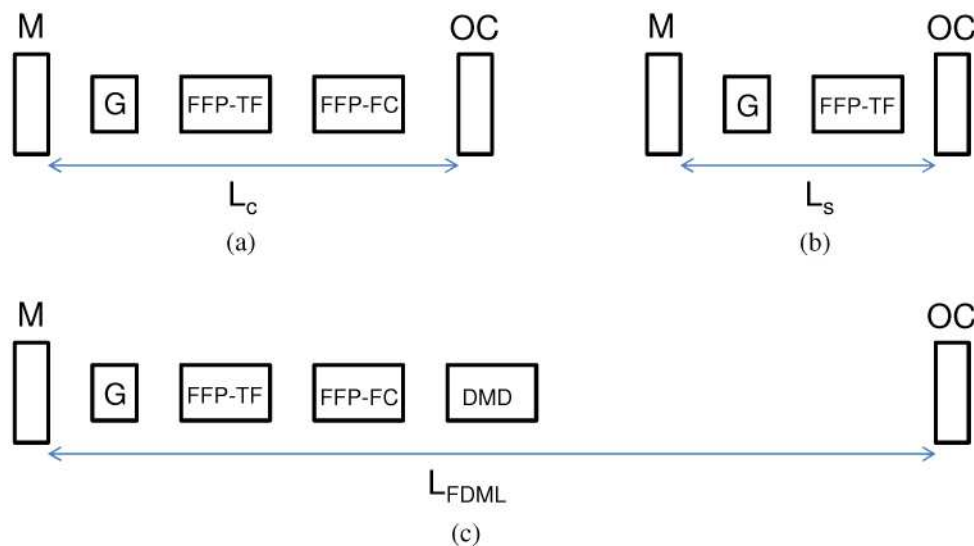


Fig. 11. FC swept laser general design: (a) standard bulk laser with two FFPs; (b) standard bulk laser with a short cavity length and one FFP; (c) FDML bulk laser with long cavity delay and two FFPs. M: mirror; OC: output coupler; G: gain medium; L: cavity length; DMD: dispersion managed delay.

## 6. Conclusion

In this study, a new type of swept laser, called a frequency comb (FC) swept laser is demonstrated which improves performance for both conventional swept lasers and FDML

lasers. The frequency comb laser generates a frequency sweep consisting of a series of frequency steps determined by an intracavity frequency comb filter. Because the frequency steps have narrower instantaneous linewidths than conventional frequency sweeping, sensitivity roll off and point spread functions are improved. It is also possible to use the filtered intensity output of the laser for self-clocking the OCT interference signal acquisition to generate a signal that is sampled with constant frequency spacing (linear in k-space).

Operation of a FC swept laser and FC-FDML laser are demonstrated at 1kHz and 120kHz sweep rates respectively over a 135nm tuning range with an average output power of 50mW. Using frequency comb operation with self clocking, the sensitivity roll off at 2.8mm delay is improved from -10dB to -1.2dB for the swept laser and from -5dB to -1.3dB for the FDML laser. Measurements at longer ranges are possible with minimum sensitivity roll off, however, reflections at depths outside the principal measurement range from 0mm to 3mm appear aliased back into the principal range. Frequency combs should improve the performance of swept source OCT for phase measurement and Doppler applications since the frequency steps in the swept laser output are precisely determined by the frequency comb filter.

The self-clocking method demonstrated in this study was performed using software sampling. Future implementations will require that special electronics be developed to enable direct clocking of high speed A/D acquisition using the filtered intensity modulated output of the frequency comb laser. However, similar improvements in performance to those reported here should be obtainable. These preliminary results also point out the importance of low timing jitter sampling for achieving good point spread functions and sensitivity roll off.

Finally, this study also presents general design rules for developing frequency comb lasers. It is interesting to note that frequency comb operation significantly improves the linewidth and sensitivity roll off performance of standard (non-FDML) swept lasers. This suggests that frequency comb (non-FDML) lasers with short cavities might achieve comparable linewidths and sensitivity performance to FDML lasers and suggests a range of new swept laser designs for OCT.

## Acknowledgements

We gratefully acknowledge the technical contributions of Drs. Benjamin Potsaid, Robert Huber and Yueli Chen. Dr. Adler is currently at LightLab Imaging, Inc. We also gratefully acknowledge technical discussions and information from Mr. Alex Cable of Thorlabs, Inc. The research was sponsored in part by the National Institute of Health R01-CA75289-12 and R01-EY011289-24; the Air Force Office of Scientific Research FA9550-07-1-0014 and Medical Free Electron Laser Program FA9550-07-1-0101. The author acknowledges support from Taiwan Merit Scholarship from the National Science Council of Taiwan and the Center for Integration of Medicine and Innovation Technology.